Applied Acoustics 127 (2017) 316–323

Contents lists available at ScienceDirect

Applied Acoustics

journal homepage: www.elsevier.com/locate/apacoust

Enhanced low- to mid-frequency sound absorption using parallel-arranged perforated plates with extended tubes and porous material

Dengke Li [a,b], Daoqing Chang [a,b,*], Bilong Liu [c]

[a] Key Laboratory of Noise and Vibration Research, Institute of Acoustics, Chinese Academy of Sciences, Beijing 100190, PR China
[b] University of Chinese Academy of Sciences, Beijing 100049, PR China
[c] School of Mechanical Engineering, Qingdao University of Technology, 777 Jialingjiang Road, Qingdao 266520, PR China

ARTICLE INFO

Article history:
Received 1 June 2017
Received in revised form 22 June 2017
Accepted 26 June 2017
Available online 10 July 2017

Keywords:
Micro-perforated plate
Perforated plate with extended tubes
Porous sound absorptive materials
Low- to mid- frequency sound absorption

ABSTRACT

Porous sound absorptive material (PSAM) and micro-perforated plate (MPP) limited by space are weak in absorbing low- to mid- frequency noise. In order to improve sound absorption in 100–1600 Hz, a compound sound absorber comprised of perforated plates with extended tubes (PPET) and a PSAM is proposed in this paper. A theoretical model is described to predict the sound absorption coefficients of two combinations: one has three parallel-arranged PPETs and a PSAM layer; the other one has two parallel-arranged PPETs, an MPP and a PSAM layer. The calculated results are then validated by the results measured in an impedance tube. The proposed combinations demonstrate superior sound absorption performance over more than three octaves in the targeted frequency range.

1. Introduction

Micro-perforated plate (MPP) is well-known for its wideband sound absorption compared to the traditional perforated plate [1–3]. The small aperture of MPP can provide sufficient resistance to improve the sound absorption and achieve wideband sound absorption. In 1975, Maa proposed the theory of MPP and presented its engineering design, which was later applied to the German Bundestag in Bonn [4]. However, when the MPP is used to control low-frequency noise, large space is required; meanwhile, the bandwidth of sound absorption is limited. To broaden the bandwidth, a double-deck MPP was further presented by Maa [2]. Later researchers proposed various constructions to improve the sound absorption of the MPP. Park [5] investigated an MPP backed by a traditional Helmholtz resonator to improve the low-frequency sound absorption and examined its applicability in reducing the noise level inside a launcher fairing. Zhao [6] investigated the combination of mechanical impedance plate with an MPP to improve the sound absorption at low frequencies. Chang [7] attached a shunt circuit containing a piezoelectric material to the MPP to improve the low- frequency sound absorption. Tao [8] greatly improved the low-frequency sound absorption of the MPP with a shunted loudspeaker. Sakagami et al. [9] studied the acoustical properties of wideband sound absorber composed of two parallel-arranged MPP absorbers, and the results showed that the impedance discontinuity between the parallel-arranged MPPs could provide extra sound absorption to broaden the sound absorption bandwidth of the MPP. By using the hybrid method of BEM and a mode expansion method, Yairi et al. [10] investigated the relationship between the extra attenuation caused by the impedance discontinuity at the boundary of the two different MPP absorbers and the sound absorption coefficient derived using the electro acoustical equivalent circuit model, and pointed out that the parallel-arrangement of MPP absorbers could obtain wideband absorption characteristics by partitioning the air cavity into sub-cavities. Recently, Wang and Huang also investigated the coupling effect of parallel-arranged MPPs with different air cavities, and concluded that multi-resonant systems have the potential to improve the bandwidth of sound absorption [11,12]. Chang and Li discussed how to design a low-frequency perforated-panel sound absorber in a space with limited thickness [13,14], focusing on the frequency range of 100–300 Hz and thickness of 100 mm, and the combination of three perforated plates with extended tubes (PPET) with one MPP were also investigated to improve the low-frequency sound absorption.

Another way of enhancing the sound absorption of MPP is the combination of perforated panel with porous materials. Li et al. [15] reported a particular design that could greatly improve the high frequency sound absorption of MPP by adding a porous layer

* Corresponding author at: Key Laboratory of Noise and Vibration Research, Institute of Acoustics, Chinese Academy of Sciences, Beijing 100190, PR China.
E-mail addresses: changdq@mail.ioa.ac.cn (D. Chang), liubl@mail.ioa.ac.cn (B. Liu).

http://dx.doi.org/10.1016/j.apacoust.2017.06.019
0003-682X/

in front of the MPP, the sound absorption coefficient is greatly improved from 500–1600 Hz when the cavity depth is not larger than 200 mm.

The aforementioned literatures show that the low-frequency sound absorption of a traditional MPP absorber could be improved by the serial or parallel coupling of micro-perforated panels and PPET, and the high-frequency sound absorption could be improved by adding a porous layer. In order to improve the sound absorption in the low- to mid- frequency range (100–1600 Hz) under the space constraint of about 100 mm depth, combinations of parallel-arranged PPETs and porous sound absorptive material (PSAM) are investigated in this paper.

The following text begins with theoretical analyses on two particular designs of PPET-PSAM absorbers (combination of three parallel-arranged PPETs and a PSAM, and combination of two parallel-arranged PPETs, an MPP and a PSAM) in Section 2, and then a parametric study of the two combinations is followed in Section 3 and experimental validation in Section 4. Lastly, conclusions are drawn in Section 5.

2. Theoretical analyses

It is noted that parallel-arranged PPETs and their combinations with MPP could achieve large sound absorption over a wider frequency range from 100 Hz to 500 Hz, while the sound absorption is greatly decreased above 500 Hz [13,14]. Thus, this paper aims at improving the sound absorption performance in the low- to mid- frequency range of 100–1600 Hz using combinations of parallel-arranged PPETs and PSAM. Two particular configurations illustrated in Fig. 1(a) and (b) are analyzed for this purpose. One configuration is composed of three parallel-arranged PPETs and a PSAM, and another one is composed of two parallel-arranged PPETs, a PSAM and an MPP.

2.1. Acoustic impedance of PPET

The construction of parallel-arranged PPETs consists of a perforated panel with a lattice of extended tubes in the back cavity, as shown in Fig. 1. The back cavity is partitioned into four subcavities with clapboards, and the cylindrical shell and clapboards are acoustically rigid. The cavity depth can be altered by changing the position of the rigid backing in the cavity.

In Fig. 1, P_i and P_r denote the incident and reflected sound waves, respectively; D is the cavity depth; t_p and t_s are the thickness of the clapboard and cylindrical shell, respectively; ϕ is the ratio of the surface-area of each component over the total area. In the following discussion, it is assumed that $\phi_1 = \phi_2 = \phi_3 = \phi_4 = 1/4$. The effective diameter of the absorber is assumed as "$d_m = 100$ mm", and the effective cross-sectional area is therefore given by "$S_m = \pi(d_m/2)^2$".

Fig. 2 illustrates one of the three parallel-arranged PPET units in Fig. 1(a). In the schematic diagram, $S_m/4$ is the cross-sectional area of this unit; t and d_0 are the length and inner diameter of the tube, respectively; r_0 and r_1 are the inner and outer radius of the extended tubes, respectively; t_0 is the thickness of the perforated panel. The specific acoustic impedance of PPET with a cavity of thickness D was derived in our previous paper [12]:

$$Z_p = \frac{Z}{\sigma_p \rho c} = r_p + j\omega m_p - j/(\delta \tan(\omega(D-t')/c) + (\delta - \sigma')\tan(\omega t'/c)) \quad (1)$$

$$r_p = \frac{32\eta t}{\sigma_p \rho c d_0^2}\left(\left(1+\frac{k^2}{32}\right)^{1/2} + \frac{\sqrt{2}kd_0}{64t}\right) \quad (2)$$

$$\omega m_p = \frac{\omega t}{\sigma_p c}\left(1+\left(9+\frac{k^2}{2}\right)^{-1/2} + 0.85\frac{d_0}{t}\right) \quad (3)$$

where η is the air viscosity, ρ is the air density, c is the sound speed in the air, ω is the angular velocity and ρc is the characteristic impedance in the air, $k = d_0\sqrt{\omega\rho/4\eta}$ is the perforation constant, "$t' = t - t_0$" is the length of extended tube inside the back cavity, "$\sigma_p = NS_0/(S_m/4)$" is the perforation ratio of the PPET, "$\delta = S_a/(S_m/4)$" is the expansion ratio of cross-sectional area from the back cavity to the PPET, and "$\sigma' = NS_1/(S_m/4)$" is the ratio of the outer cross-sectional area of the extended tubes over that of the PPET (N denotes the number of extended tubes, "$S_0 = \pi r_0^2$" is the inner cross-sectional area of the extended tubes, S_a is the effective cross-sectional area of the back cavity, "$S_1 = \pi r_1^2$" is the outer cross-sectional area of the extended tube). When "$t' = 0$", the extended tubes are absent and the cavity reactance is "$z_D = -j\cot(\omega D/c)/\delta$". When "$t' = D$", the extended tubes reach the rigid backing and the cavity reactance is "$z_D = -j\cot(\omega D/c)/(\delta - \sigma')$".

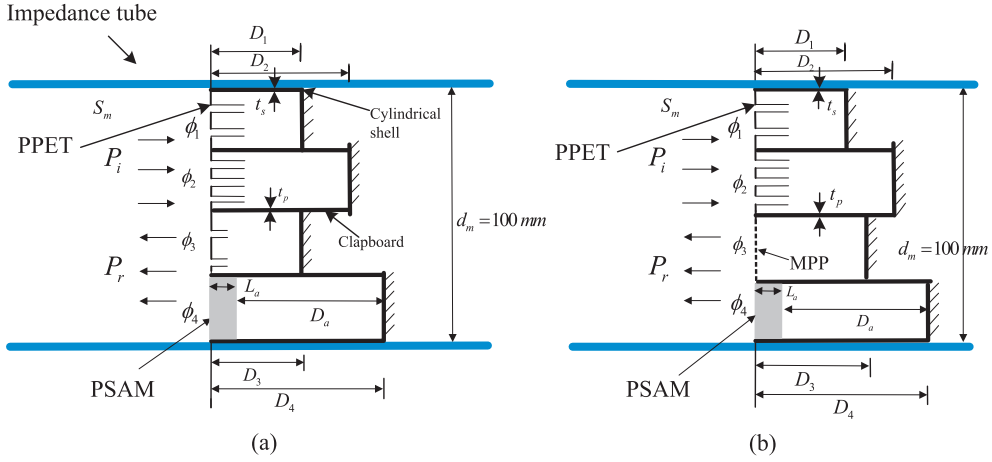

Fig. 1. Schematic diagrams of two constructions of the proposed compound sound absorber: (a) three parallel-arranged PPETs and a PSAM; (b) two parallel-arranged PPETs combined with an MPP and a PSAM.

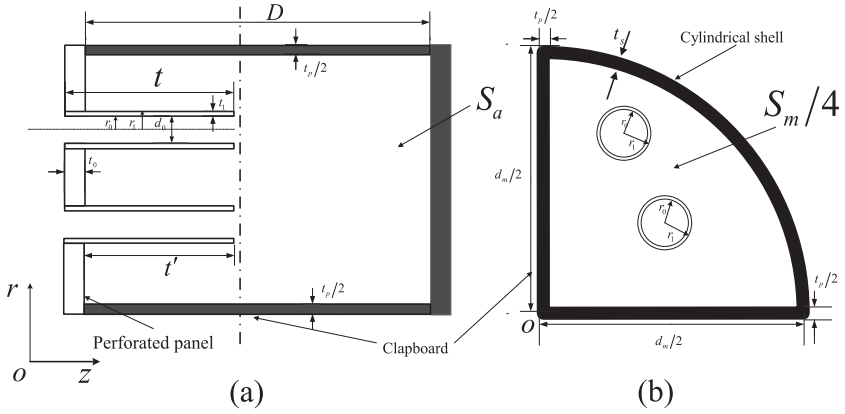

Fig. 2. Schematic diagrams of one unit of the three parallel-arranged PPETs: (a) side elevation; (b) front elevation.

2.2. Acoustic impedance of PSAM

The semi-empirical Delany-Bazley (DB) model is adopted to predict the sound absorption of high-porosity fibrous materials [16], and the Dunn-Davern (DD) model is adopted to predict the sound absorption of high-porosity foam materials [17].

$$z_a = \rho c\left[1 + c_1\left(\rho\frac{f}{R_a}\right)^{c_2} - jc_3\left(\rho\frac{f}{R_a}\right)^{c_4}\right] \tag{4}$$

$$k_p = \frac{\omega}{c}\left[1 + c_7\left(\rho\frac{f}{R_a}\right)^{c_8} - jc_5\left(\rho\frac{f}{R_a}\right)^{c_6}\right] \tag{5}$$

where R_a, z_a and k_p are the resistivity, characteristic impedance and wave number of the PSAM, respectively, f is the frequency of the sound wave, and ρ is the air density, c is the sound speed in the air, ω is the angular velocity. The 8 parameters required in the DB and DD model are listed in Table 1.

The acoustic impedance of the back cavity of the PSAM is

$$Z_D = -j\rho c\cot\left(\frac{\omega}{c}D_a\right) \tag{6}$$

where D_a is the cavity depth. According to the impedance transfer formula, the surface acoustic impedance of the PSAM is then given by

$$Z_{psam} = z_a\frac{Z_D + jz_a\tan(k_pL_a)}{z_a + jZ_D\tan(k_pL_a)} \tag{7}$$

where L_a is the thickness of PSAM. The relative acoustic impedance of PSAM can be written as

$$Z_{PSAM} = Z_{psam}/(\rho c) \tag{8}$$

2.3. Acoustic impedance of MPP

According to Maa [1], the relative acoustic impedance of an MPP with back cavity depth D_{mpp} is

$$Z_{mpp} = r_{mpp} + j\omega m_{mpp} - j\cot\left(\frac{\omega}{c}D_{mpp}\right) \tag{9}$$

$$r_{mpp} = (32\eta t_{mpp}/\sigma_{mpp}\rho c d_{mpp}^2)((1 + k^2/32)^{1/2} + (\sqrt{2}kd_{mpp}/32t_{mpp})) \tag{10}$$

$$\omega m_{mpp} = (\omega t_{mpp}/\sigma_{mpp}c)(1 + (9 + k^2/2)^{-1/2} + 0.85d_{mpp}/t_{mpp}) \tag{11}$$

where $k = d_{mpp}\sqrt{\omega\rho/4\eta}$ is the perforation constant, t_{mpp}, d_{mpp}, σ_{mpp} and D_{mpp} are the thickness, diameter, perforation ratio and cavity depth of MPP, respectively.

2.4. Sound absorption coefficients of the two PPET-PSAM combinations

For the combination of three PPETs and a PSAM (Fig. 1(a)), the acoustic impedance of the composite absorber can be derived by

$$Z = \left(\frac{\phi_1}{Z_{p1}} + \frac{\phi_2}{Z_{p2}} + \frac{\phi_3}{Z_{p3}} + \frac{\phi_4}{Z_{PSAM}}\right)^{-1} \tag{12}$$

where Z_{P1}, Z_{P2}, Z_{P3}, and Z_{PSAM} are the acoustic impedances of PPET1, 2, 3 and PSAM, respectively.

For the combination of two PPETs, an MPP and a PSAM (Fig. 1(b)), the acoustic impedance can be written as

$$Z = \left(\frac{\phi_1}{Z_{p1}} + \frac{\phi_2}{Z_{p2}} + \frac{\phi_3}{Z_{MPP}} + \frac{\phi_4}{Z_{PSAM}}\right)^{-1} \tag{13}$$

where Z_{P1}, Z_{P2}, Z_{MPP}, and Z_{PSAM} are the acoustic impedance of PPET1, 2, MPP and PSAM, respectively.

Finally, the normal-incidence sound absorption coefficient is given by

$$\alpha = \frac{4Real(Z)}{(1 + Real(Z))^2 + (Imag(Z))^2} \tag{14}$$

3. Results and discussions

3.1. Sound absorption of the combination of three parallel-arranged PPETs and a PSAM

The sound absorption coefficient of the combination of three parallel-arranged PPETs and a PSAM (glass wool) is plotted in

Table 1
Eight parameters in the DB and DD model.

Parameters	c_1	c_2	c_3	c_4	c_5	c_6	c_7	c_8
DB model	0.0571	−0.754	−0.087	−0.732	0.189	−0.595	0.0978	−0.7
DD model	0.144	−0.369	−0.985	−0.758	0.168	−0.715	0.136	−0.491

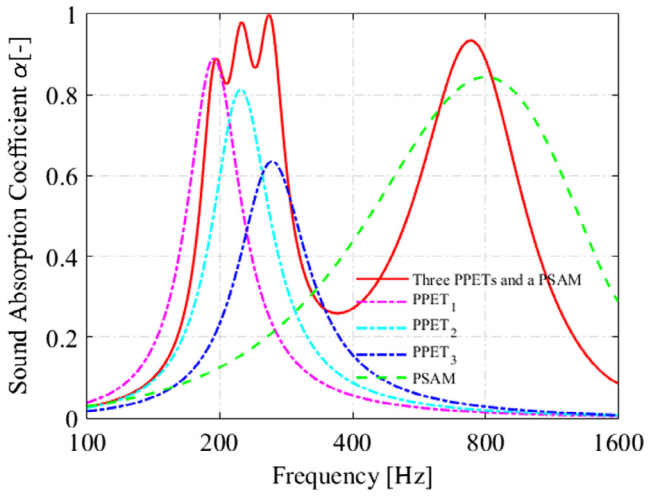

Fig. 3. Sound absorption coefficients of three parallel-arranged PPETs and a PSAM (glass wool).

Fig. 3, and the sound absorption coefficients of the three PPETs and PSAM are also shown for comparison. The thicknesses of the perforated panel, the clapboard, the cylindrical shell and the extended tube are 2 mm, 4 mm, 4 mm and 0.5 mm, respectively, and the parameters of the three PPETs and a PSAM are listed in Table 2. In a recent study of the present authors [14], parallel-arranged PPETs could achieve an average sound absorption coefficient of 0.85 at the frequencies 100–300 Hz. In an attempt to improve the sound absorption above 300 Hz, a thin PSAM combined with the same back cavity is introduced in this paper. It could be observed from Fig. 3 that the sound absorption coefficient of the combination is also high at the sound absorption peak of each single PPET and PSAM. Three absorption peaks observed at 195 Hz, 222 Hz and 259 Hz are caused by the Helmholtz resonances of the PPETs, while the resonance of the PSAM contributes to the forth peak observed at 744 Hz. It is noted in Fig. 3 that the sound absorption of the combination in the mid-frequency range (300–1200 Hz) is improved notably by the PSAM; hence the combination can greatly improve the sound absorption at low frequencies and maintain reasonably high sound absorption in the mid-frequency range.

Note that the parameters of both PPET components and PSAM will greatly influence the sound absorption of the combination, so a parametric study of the combination is investigated in the next subsection.

3.2. Parametric study of the combination of three parallel-arranged PPETs and a PSAM

Note that for this combination, the parameters of each PPET and PSAM can influence the overall sound absorption performance. In this pilot study, the following aspects are investigated: the effects of the resistivity of the PSAM, the inner diameters and lengths of the tubes of the three PPETs, and the surface-area occupation ratio of each PPET and PSAM on the overall sound absorption performance of the combination.

Fig. 4(a) shows the effect of the resistivity of PSAM on the sound absorption of this combination. It could be observed from Fig. 4(a) that with the increase of resistivity from 2175 to 6175 Pa · s/m^2, the sound absorption is improved in the frequency range from 300 Hz to 700 Hz. When the resistivity is 2175 Pa · s/m^2, the acoustic characteristic resistance is too small to enhance both sound absorption coefficient and absorption bandwidth. In contrast, when the resistivity is 12,175 Pa · s/m^2, the acoustic characteristic resistance is so large that the sound absorption peaks are greatly reduced. Hence a moderate resistivity is normally required to enhance the sound absorption performance.

Fig. 4(b) shows the effect of the inner diameter of the extended tube on the sound absorption of this combination. When the tube diameter is 2 mm, the sound absorption peaks of the PPETs are greatly reduced because the characteristic acoustic resistance of the tube is too large to achieve high sound absorption. In contrast, when the diameter of the extended tube is 7 mm, the characteristic acoustic resistance of the tube is too small to maintain a satisfactory sound absorption bandwidth. Hence a moderate tube diameter is also required to enhance the sound absorption performance.

Fig. 4(c) compares the variation of the tube length of PPETs on the sound absorption of this combination. Increasing the tube length will greatly shift the resonance frequency to a lower frequency because of the increased acoustic mass reactance, and then the sound absorption peaks of the PPETs are shifted to lower frequencies.

Fig. 4(d) illustrates the variation of the surface-area occupation ratio of each PPET and PSAM on the sound absorption of this combination. When the occupation ratio of the PSAM changes from 0.25 to 0.5, the sound absorption is improved in the frequency range from 400 Hz to 1600 Hz, while the absorption peaking belonging to the three PPETs decrease slightly.

3.3. Sound absorption of the combination of two parallel-arranged PPETs, an MPP and a PSAM

In this subsection, the same method is applied to analyze how two parallel-arranged PPETs and a PSAM could further improve the sound absorption of a traditional MPP absorber. A schematic diagram of such combination is shown in Fig. 1(b). The thicknesses of the perforated panel, the MPP, the clapboard, the cylindrical shell and the extended tube are 2 mm, 2 mm, 4 mm, 4 mm and 0.5 mm, respectively. The derived sound absorption coefficient and normalized acoustic impedance of this combination are shown in Fig. 5, where the optimized MPP and single PSAM layer are also shown for comparison. The parameters of the two PPETs, an MPP and a PSAM are listed in Table 3. The optimized parameters of a single MPP and PSAM layer are obtained by optimizing the average sound absorption coefficient over the frequency range of 100–1600 Hz with the simulated annealing method [14].The sound absorption peak at each resonance frequency is well above 0.9, and the reactance of the combination is near zero around the res-

Table 2
Parameters for three parallel-arranged PPETs and a PSAM.

Samples	$PPET_1$					$PPET_2$				
Parameters	d_1(mm)	t_1(mm)	σ_1(%)	D_1(mm)	ϕ_1(−)	d_2(mm)	t_2(mm)	σ_2(%)	D_2(mm)	ϕ_2(−)
	4.0	40	3.84	85	0.25	4.0	40	5.15	88	0.25
Samples	$PPET_3$					PSAM (glass wool)				
Parameters	d_3(mm)	t_3(mm)	σ_3(%)	D_3(mm)	ϕ_3(−)	L_a(mm)	R_a(Pa.s/m^2)		D_a(mm)	ϕ_4(−)
	4.0	20	4.48	99	0.25	20	6175		85	0.25

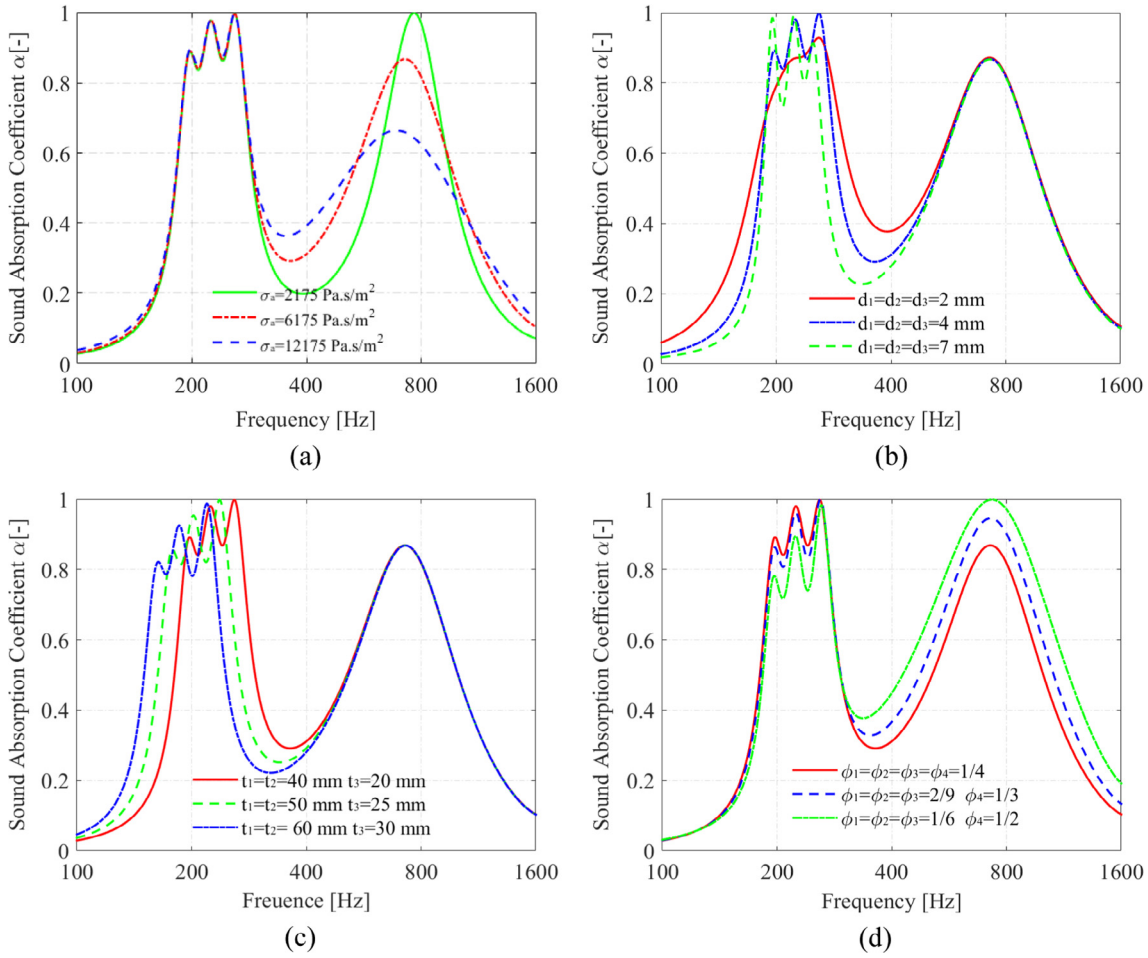

Fig. 4. Influences of different parameters on the sound absorption efficient of the combination of three parallel-arranged PPETs and a PSAM (glass wool): (a) influence of the resistivity of the PSAM; (b) influence of the tube diameter of the three PPETs; (c) influence of the tube length of the three PPETs; (d) influence of the surface-area occupation of the three PPETs and the PSAM.

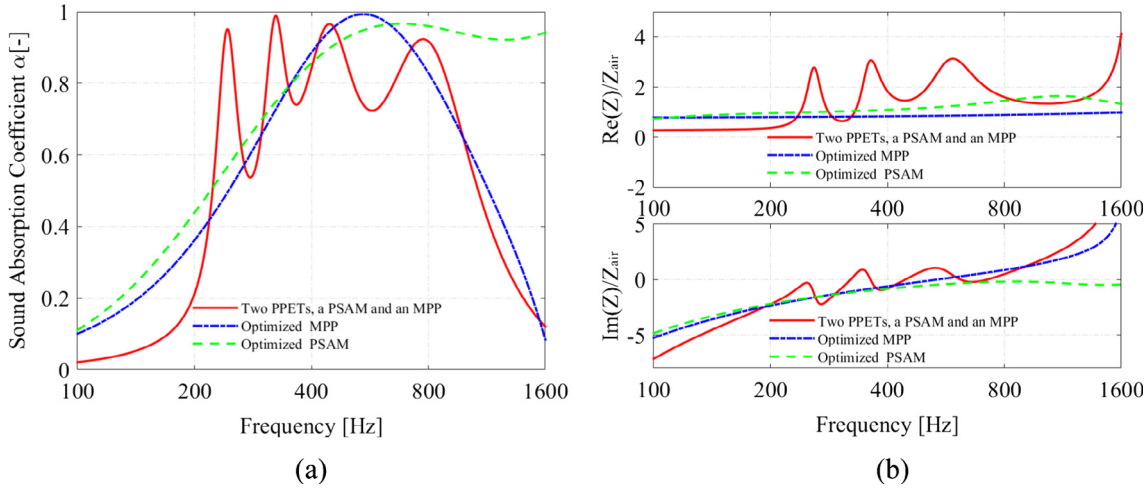

Fig. 5. Sound absorption coefficients of the combination of two parallel-arranged PPETs, an MPP and a PSAM (glass wool): (a) sound absorption coefficient; (b) normalized acoustic characteristic impedance. The parameters of the single optimized PPET are as follows: $d_1 = 0.5$ mm, $t_1 = 3$ mm, and $\sigma_1 = 5.1\%$. The parameters of the optimized single PSAM are as follows: $L_a = 100$ mm and $R_a = 9864$ Pa.s/m^2.

onance frequency at 243 Hz, 324 Hz, 445 Hz and 775 Hz. The first two peaks correspond to the resonances of the PPETs, the third sound absorption peak to the resonance of the MPP, and the forth peak observed at 776 Hz to the resonance of the PSAM. The combination can achieve sound absorption coefficient larger than 0.5 over a wide band from 220 Hz to 1100 Hz, and the effective sound absorption bandwidth is about 740 Hz (with sound absorption coefficient larger than 0.7).

Table 3
Parameters for two parallel-arranged PPETs combined with a PSAM and an MPP.

Samples	$PPET_1$					$PPET_2$				
Parameters	d_1(mm)	t_1(mm)	σ_1(%)	D_1(mm)	ϕ_1(−)	d_2(mm)	t_2(mm)	σ_2(%)	D_2(mm)	ϕ_2(−)
	4.0	40	5.76	85	0.25	4.0	20	5.76	86	0.25
Samples	MPP					PSAM (glass wool)				
Parameters	d_3(mm)	t_3(mm)	σ_3(%)	D_3(mm)	ϕ_3(−)	L_a(mm)	R_a(Pa.s/m^2)		D_a(mm)	ϕ_4(−)
	1.0	2.0	2.16	100	0.25	20	6175		78	0.25

Compared with the optimized MPP, the combination has much better performance in the frequency range from 215 Hz to 460 Hz because the couplings between two PPETs, an MPP and a PSAM could lead to acoustic reactance matching at more frequency points to expand the bandwidth of effective sound absorption, as illustrated in Fig. 5. Moreover, the combination has better performance than a traditional PSAM below 500 Hz. Note that in this frequency range, it is impossible to achieve satisfactory sound absorption performance using a single PSAM with limited thickness. It could be concluded that the construction of parallel-arranged PPETs combined with a PSAM have better potential to improve the sound absorption performance of a traditional MPP.

4. Experiment validations

The sound absorption coefficients and impedances of the aforementioned two combinations are tested according to the ISO 10534-2 [18] in an impedance tube (B&K 4206) with inner diameter of 100 mm. Each test sample is installed inside the impedance tube in the way shown in Fig. 6. The perforated panels used in the experiments are plastic plate and the extended tubes are made of copper. The thickness of the perforated panel, extended tubes and micro-perforated panel are 2 mm, 0.5 mm and 2 mm, respectively. Two kinds of porous materials are tested in the experiments: one is the glass wool with resistivity of $R_a = 6175$ Pa.s/m^2 and the other one is the melamine foam with resistivity of $R_a = 7886$ Pa.s/m^2. The resistivity of the porous material is tested according to the ISO 9053 [19]. The clapboard and cylindrical shell of the back cavity are 4 mm in thickness.

The parameters used for the combination of three parallel-arranged PPETs and a PSAM are listed in Tables 2 and 4, while the parameters used for the combination of two parallel-arranged PPETs, an MPP and a PSAM are listed in Tables 3 and 5. The measured results are shown in Fig. 7 and Fig. 8, reasonable agreement is found between the predicted and measured sound absorption curves and normalized characteristic impedance curves. The results of the samples with glass wool as the porous layer are shown in Fig. 7(a) and Fig. 8(a), and the results of those with melamine foam are shown in Fig. 7(b) and Fig. 8(b). It could be seen in Fig. 7 that the measured sound absorption peaks of the combination of three parallel-arranged PPETs and glass wool is well above 0.9 and the effective sound absorption bandwidth is about 400 Hz, while the resonance peaks of the combination of three parallel-arranged PPETs and melamine foam are well above 0.8 and the effective sound absorption bandwidth is about 430 Hz.

Furthermore, the sound absorption performance can be further improved by the combination with an MPP, as plotted in Fig. 8. For the combination of two parallel-arranged PPETs, an MPP and glass wool, the sound absorption coefficient is well above 0.5 from 225–1100 Hz, and the measured effective sound absorption bandwidth is about 740 Hz. For the combination of two parallel-arranged PPETs, an MPP and melamine foam, the sound absorption coefficient is well above 0.5 from 240–1200 Hz, and the measured effective sound absorption bandwidth is about 820 Hz. The measured results show that large sound absorption in the low- to mid- frequency range is achieve by an absorber construction with limited thickness of 100 mm.

In general, errors between the calculated and measured results may occur when the resonance peaks are coupled together, or at the anti-resonance peaks. It is worth mentioning that the perforated panel and the back cavity must be well-sealed to observe the resonance peaks of the PPETs and MPP.

5. Conclusions

In this paper, the feasibility of combining parallel-arranged perforated plates with extended tubes (PPETs) with porous sound absorptive material (PSAM) to improve the sound absorption performance at low- to mid- frequencies (100–1600 Hz) is investigated theoretically and experimentally. A theoretical model is described to predict the sound absorption of two combinations: one has three parallel-arranged PPETs and a PSAM layer, and effective sound absorption is achieved in the low frequency range of 180–350 Hz and the middle frequency range of 600–900 Hz; the

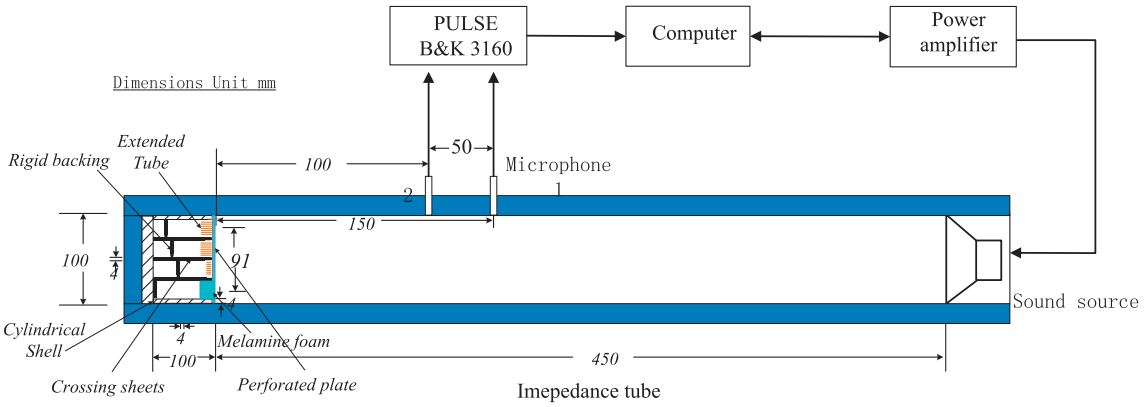

Fig. 6. The experimental set up.

Table 4
Parameters of the combination of three parallel-arranged PPETs and a PSAM.

Samples	$PPET_1$					$PPET_2$				
Parameters	d_1(mm)	t_1(mm)	σ_1(%)	D_1(mm)	ϕ_1(−)	d_2(mm)	t_2(mm)	σ_2(%)	D_2(mm)	ϕ_2(−)
	3.2	40	3.69	74	0.25	4.0	40	5.15	70	0.25
Samples	$PPET_3$					PSAM (melamine Foam)				
Parameters	d_3(mm)	t_3(mm)	σ_3(mm)	D_3(mm)	ϕ_3(−)	L_a(mm)	R_a(Pa.s/m^2)		D_a(mm)	ϕ_4(−)
	4.0	20	4.48	70	0.25	20	7886		85	0.25

Table 5
Parameters of the combination of two parallel-arranged PPETs, an MPP and a PSAM.

Samples	$PPET_1$					$PPET_2$				
Parameters	d_1(mm)	t_1(mm)	σ_1(%)	D_1(mm)	ϕ_1(−)	d_2(mm)	t_2(mm)	σ_2(%)	D_2(mm)	ϕ_2(−)
	4.0	40	5.76	70	0.25	4.0	20	5.76	80	0.25
Samples	MPP					PSAM (melamine Foam)				
Parameters	d_3(mm)	t_3(mm)	σ_3(%)	D_3(mm)	ϕ_3(−)	L_a(mm)	R_a(Pa.s/m^2)		D_a(mm)	ϕ_4(−)
	1.0	2.0	1.72	84	0.25	20	7886		70	0.25

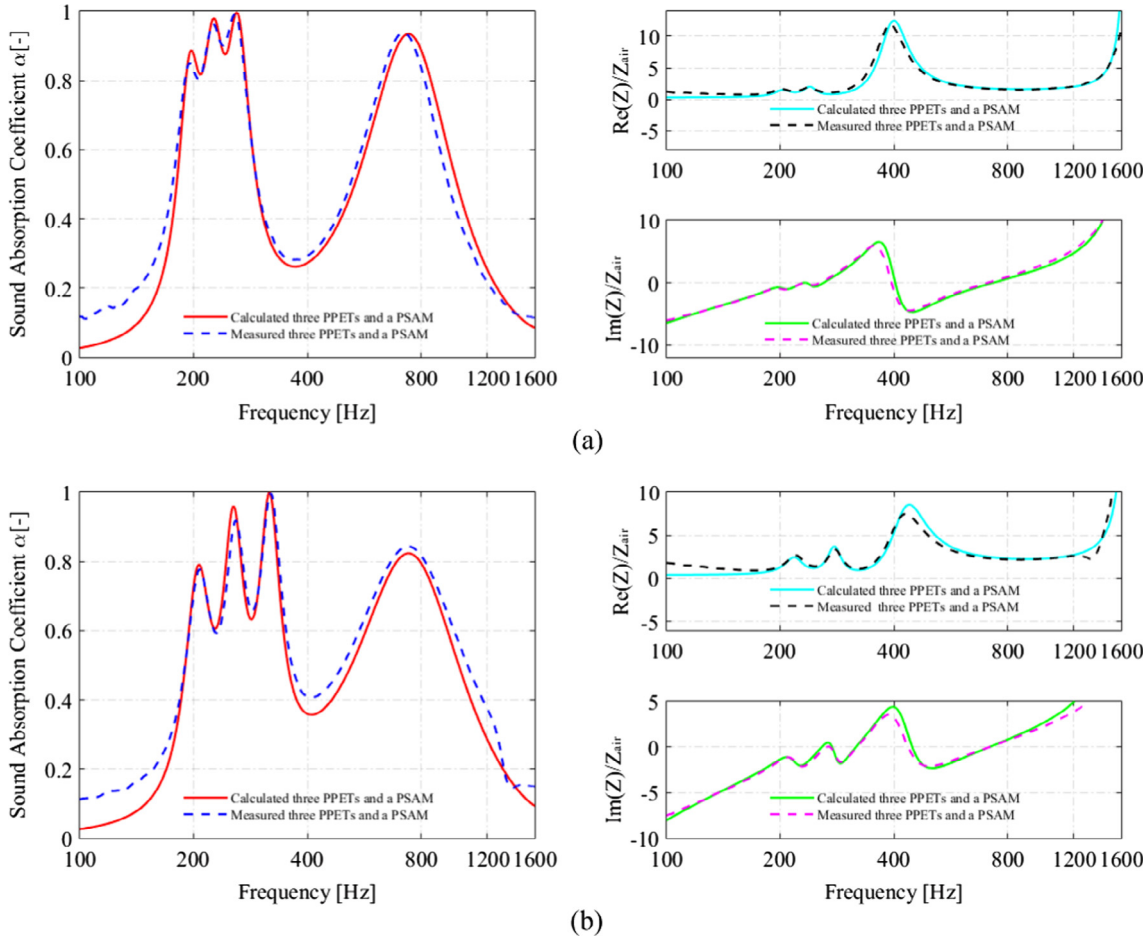

Fig. 7. Comparison of the calculated and measured results for the combination of three parallel-arranged PPETs and a PSAM: (a) the PSAM is glass wool, and the parameters are listed in Table 2; (b) the PSAM is melamine foam, and the parameters are listed in Table 4. The red solid line and the blue dashed line represent the calculated and measured sound absorption coefficient, respectively; the cyan solid line and the black dashed line represent the calculated and measured normalized characteristic resistance curves, respectively; the green solid line and the pink dashed line represent the calculated and measured normalized characteristic reactance curves, respectively. (For interpretation of the references to colour in this figure legend, the reader is referred to the web version of this article.)

other one has two parallel-arranged PPETs, an MPP and a PSAM layer, and effective sound absorption is achieved from 230 Hz to 1k Hz. The predicted results agree well with the results measured in an impedance tube. Compared with the conventional absorbers, the proposed combinations show much better sound absorption performance in the low- to middle- frequency range. Hence the method described in this paper is useful for the design of sound absorber at low- to mid- frequencies.

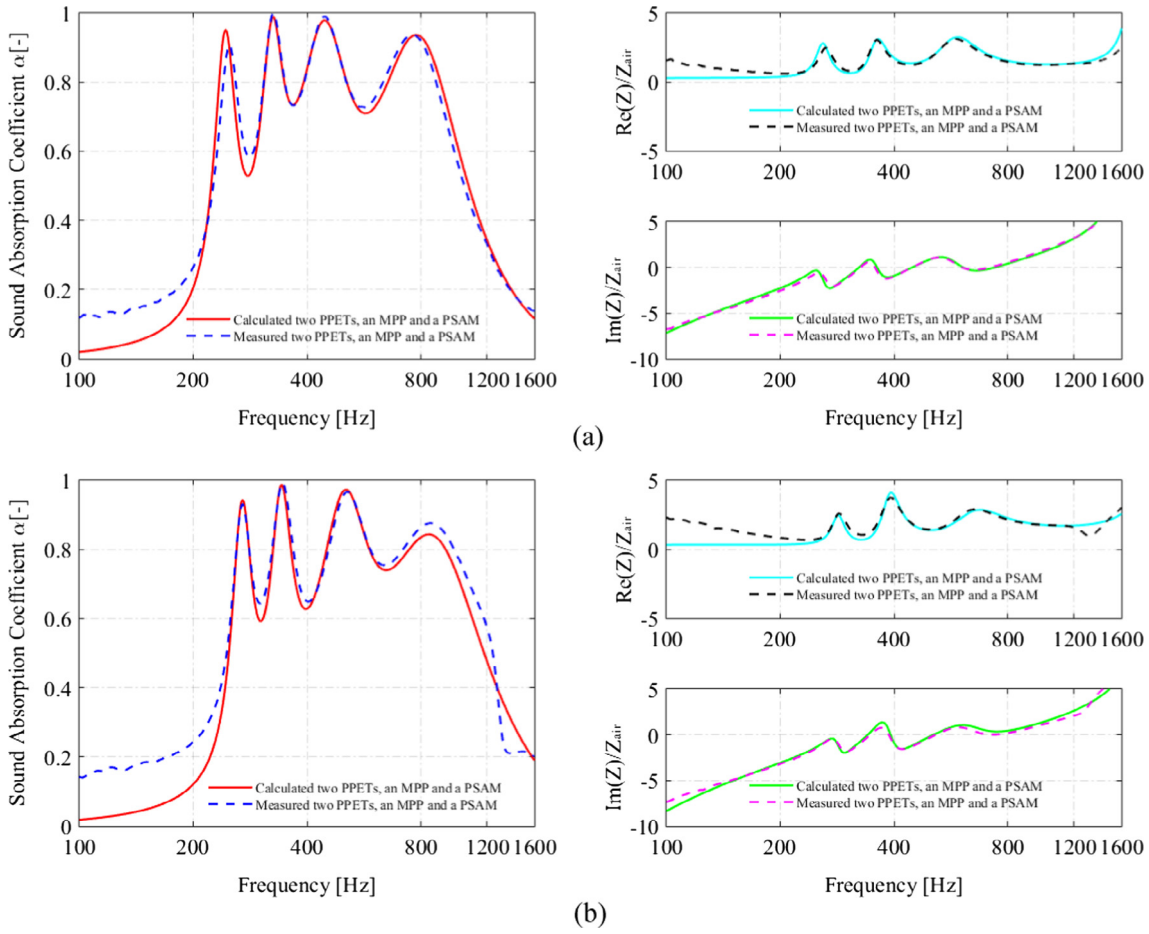

Fig. 8. Comparison of the calculated and measured results for the combination of two parallel-arranged PPETs, an MPP and a PSAM: (a) the PSAM is glass wool, and the parameters are listed in Table 3; (b) the PSAM is melamine foam, and the parameters are listed in Table 5. The red solid line and the blue dashed line represent the calculated and measured sound absorption coefficient, respectively; the cyan solid line and the black dashed line represent the calculated and measured normalized characteristic resistance curves, respectively; the green solid line and the pink dashed line represent the calculated and measured normalized characteristic reactance curves, respectively. (For interpretation of the references to colour in this figure legend, the reader is referred to the web version of this article.)

Acknowledgement

This work is supported by the National Natural Science Foundation of China (Grant No. 11374326). We would like to thank them for their assistance. The first author is also grateful for the scholarship from the China Scholarship Council.

References

[1] Maa DY. Theory and design of micro-perforated sound absorbing constructions. Scientia Sinca 1975;18:55–71.
[2] Maa DY. Microperforated-panel wideband absorbers. Noise Control Eng J 1987;29:77–84.
[3] Maa DY. Practical single MPP absorber. Int J Acoust Vib 2007;12:3–6.
[4] Fuches HV, Zha XQ. Acrylic-glass sound absorbes in the pleum of dentscher bundstag. Appl Acoust 1997;52:211–7.
[5] Park SH. Acoustic properties of micro-perforated panel absorbers backed by Helmholtz resonators for the improvement of low-frequency sound absorption. J Sound Vib 2013;332:4895–911.
[6] Zhao XD, Fan XQ. Enhancing low frequency sound absorption of micro-perforated panel absorbers by using mechanical impedance plates. Appl Acoust 2015;88:123–8.
[7] Chang DQ, Liu BL, Li XD. An electromechanical low frequency panel sound absorber. J Acoust Soc Am 2010;128:639–45.
[8] Tao JC, Jing RX, Qiu XJ. Sound absorption of a finite micro-perforated plate backed by a shunted loudspeaker. J Acoust Soc Am 2013;135:231–8.
[9] Sakagami K, Nagayama Y, Morimoto M, Yairi M. Pilot study on wideband sound absorber obtained by combination of two different micro-perforated panel (MPP) absorbers. Acoust Sci Tech 2009;30(2):154–6.
[10] Yairi M, Sakagami K, Takebayashi K, Morimoto M. Excess sound absorption at normal incidence by two micro-perforated panel absorbers with different impedance. Acoust Sci Tech 2011;32(5):194–200.
[11] Wang CQ, Huang LX. On the acoustic properties of parallel arrangement of multiple micro-perforated panels with different cavity depths. J Acoust Soc Am 2010;130:208–18.
[12] Wang CQ, Huang LX, Zhang YM. Oblique incidence sound absorption of parallel arrangement of multiple micro-perforated panels in a periodic pattern. J Sound Vib 2014;333:6828–42.
[13] Li DK, Chang DQ, Liu BL, Tian J. A perforated panel sound absorber for low frequencies. In: Proceedings of 22nd international congress on sound and vibration, Florence, Italy, July 12–16; 2015.
[14] Li DK, Chang DQ, Liu BL. Enhancing the low frequency sound absorption of a perforated panel by parallel-arranged extended tubes. Appl Acoust 2016;102:126–32.
[15] Li DK, Chang DQ, Liu BL. Tian J. Improving the sound absorption bandwidth of micro-perforated panel by adding porous sound absorbing materials. In: Proceedings of internoise 2014, Melbourne, Australia; 2014.
[16] Delany ME, Bazley EN. Acoustical properties of fibrous absorbent materials. Appl Acoust 1970;3:105–16.
[17] Dunn IP, Davern WA. Calcualtion of the multilayer absorbers. Appl Acoust 1986;19:321–34.
[18] ISO 10524–2. Acoustics – Determination of sound absorption coefficient and impedance in impedance tubes – Part 2: Transfer function method; 1998.
[19] ISO 9053. Acoustics – Materials for acoustical application – determination of airflow resistance; 1991.